From the Department of Cell and Molecular Biology
Karolinska Institutet, Stockholm, Sweden

MOLECULAR ORGANIZATION AND IN SITU ASSEMBLY OF THE HUMAN SKIN BARRIER

Lianne den Hollander

Karolinska Institutet

Stockholm 2016

Somewhere, something incredible is waiting to be known.

Carl Sagan

Molecular organization and in situ assembly of the human skin barrier

THESIS FOR DOCTORAL DEGREE (Ph.D.)

by

Lianne den Hollander

Principal Supervisor:
Dr Lars Norlén
Karolinska Institutet
Department of Cell and Molecular Biology

Co-supervisor(s):
Professor Bertil Daneholt
Karolinska Institutet
Department of Cell and Molecular Biology

Opponent:
Professor Philip Wertz
University of Iowa
Department of Oral Pathology, Radiology and Medicine

Examination Board:
Professor Klas Nordlind
Karolinska Institutet
Department of Medicine

Professor Johan Engblom
Malmö University
Department of Biomedical Sciences

Professor Oleg Shupliakov
Karolinska Institutet
Department of Neuroscience

ABSTRACT

A deficient skin barrier function is a characteristic feature of skin diseases such as eczema, psoriasis and the ichtyoses. A malformation of the lipid matrix might be a major factor in barrier deficient skin disease. To better understand barrier function impairments in the future we studied the in situ assembly and molecular organization of the healthy skin barrier.

Presently, two different models for the lipid secretion system, lamellar body system, have been proposed – the Landmann model and the membrane-folding model. The Landmann model proposes lipid secretion into the extracellular space between viable and cornified epidermis via a diffusion/fusion based process of multiple discrete lipid containing vesicles, while the membrane folding model proposes lipid secretion via a single and coherent continuous tuboloreticular system associating the cytoplasmic transGolgi with the extracellular space.

In this thesis the continuity versus discreteness of the lamellar body system was addressed with three complementary 3D electron microscopy methodologies - tomography of vitreous sections (TOVIS), freeze-substitution serial section electron tomography (FS-SET) and focused ion beam scanning electron microscopy (FIB-SEM) tomography, using cryo-electron microscopy of vitreous sections (CEMOVIS) as a high-resolution 2D reference. We show that lamellar bodies are not discrete vesicles but part of a tubuloreticular membrane network filling out a large portion of the cytoplasm and being continuous with the plasma membrane of stratum granulosum cells.

The next step in skin barrier formation is the lipid molecular assembly. We found five different characteristic high-resolution CEMOVIS patterns that correspond to five different steps in the lipid reorganization process. Using a novel approach combining very-high magnification cryo-electron microscopy of vitreous skin section (CEMOVIS) defocus-series, molecular modelling and electron microscopy simulation we determined the molecular organisation of the lipid matrix in each of the five steps. We conclude that the human skin barrier is formed by a cubic-to-lamellar lipid bilayer phase transition followed by a rearrangement of the ceramide hydrocarbon chains from a hairpin-like to a fully splayed conformation with a concomitant displacement of cholesterol from symmetric to asymmetric distribution between lipid layers.

Finally we show with the same novel approach that when the skin barrier formation is complete, the lipid matrix is organized as asymmetrical stacked bilayers of fully extended ceramides with cholesterol associated to the ceramide sphingoid moiety. This rationalizes the skin's low permeability towards both water and towards hydrophilic and lipophilic substances, as well as the skin barrier's robustness towards hydration and dehydration, environmental temperature and pressure changes, stretching, compression, bending and shearing.

The near-native high resolution molecular description of skin barrier and its formation presented in this thesis opens the door for molecular dynamics modelling as well as in-vitro modelling, of barrier function and its deficiency in normal and diseased skin.

LIST OF SCIENTIFIC PAPERS

I. **The human skin barrier is organized as stacked bilayers of fully extended ceramides with cholesterol molecules associated with the ceramide sphingoid moiety.**

Iwai I, Han HM*, **den Hollander L***, Svensson S, Öfverstedt LG, Anwar J, Brewer J, Bloksgaard M, Laloeuf A, Nosek D, Masich S, Bagatolli LA, Skoglund U, Norlén L. (2012) *J Invest Dermatol* 132: 2215-25.
* These authors contributed equally

II. **Skin Lamellar Bodies are not Discrete Vesicles but Part of a Tubuloreticular Network.**

den Hollander L, Han HM, de Winter M, Svensson L, Masich S, Daneholt B, Norlén L. (2016) *Acta Derm Venereol* 96: 303-8.

III. **The stepwise formation of the human skin barrier examined in situ on the molecular level.**

den Hollander L*, Narangifard A*, Iwai I, Han HM, Wennberg C, Lundborg M, Masich S, Daneholt B, Norlén L.
* These authors contributed equally

CONTENTS

LIST OF ABBREVIATIONS

HPF	High pressure freezing
FS	Freeze-substitution
FS-SET	Freeze-substitution serial electron tomography
CEMOVIS	Cryo electron microscopy of vitreous sections
TOVIS	Tomography of vitreous sections
FIB-SEM	Focus ion beam scanning electron microscopy
QDs	Quantum dots

1 INTRODUCTION

1.1 THE SKIN

The human skin is the largest and heaviest organ of the human body. The skin forms a physical barrier between body and the environment and is our first line of defense against external hazards. At the same time it controls thermal regulation by an extended blood vessel and sweating system and with its variety of nerve endings it forms one of our seven senses. For the average adult, the skin covers an area of approximately 2 m^2 and has a thickness varying between 1-10 mm. (McGrath et al., 2004; Proksch et al., 2008)

The skin is composed of two anatomical layers: epidermis and dermis (Fig. 1). The epidermis is the outermost, cornified layer of the skin and is responsible for the barrier function of our skin. The dermis consists of a dense fibro-elastic matrix tissue containing nerve endings, sweat glands, blood vessels and hair follicles. Both layers rest on a viscoelastic bed composed of loose fatty connective tissue, the hypodermis or subcutis. This loose fatty connective tissue serves to dissipate mechanical stress inflicted on the skin, as an insulated layer and attaches the skin to the underlying bone structure (McGrath et al., 2004).
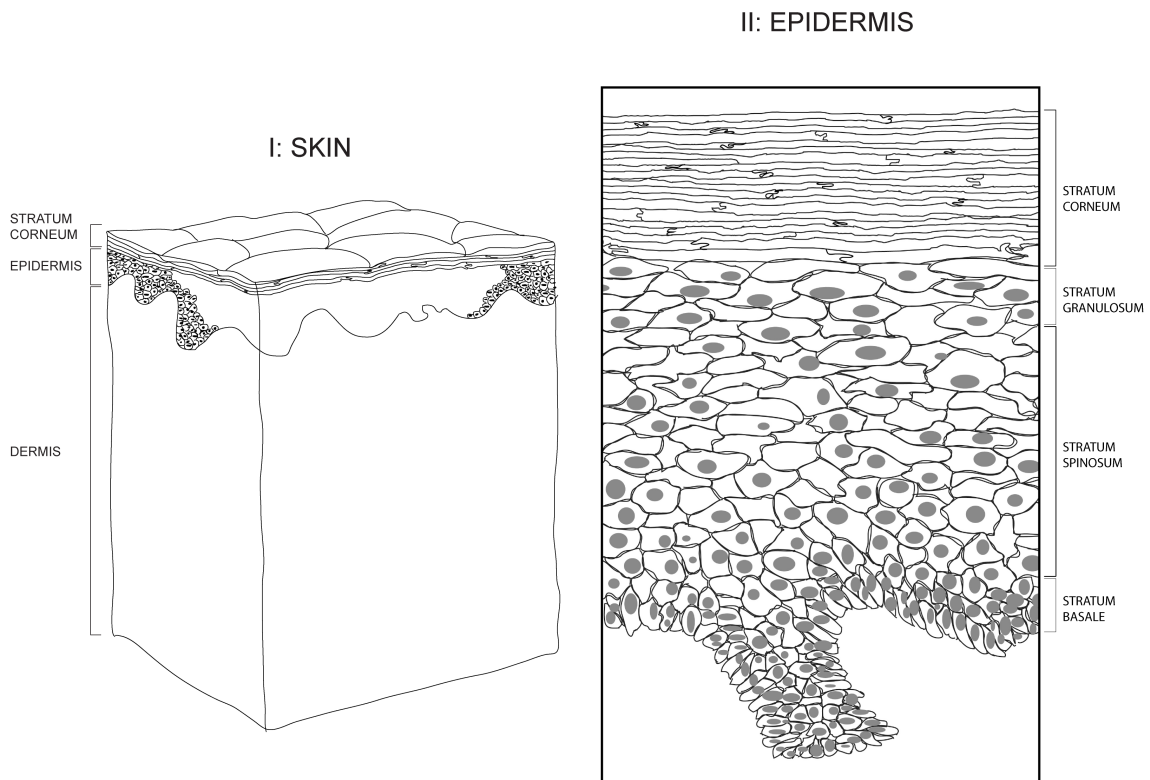

Fig 1. **Overview of the ultrastructure of the human skin.** Section I: organ-scale drawing of the skin. Section II: tissue-scale drawing of the epidermis with its different layers.

1.1.1 Epidermis

The epidermis is a stratified keratinizing epithelium composed of an outer layer of anucleated dead cornified cells, the stratum corneum, and living inner cell layers. The epidermis can be further subdivided into four sub-layers: a) stratum basale, which is primarily made up of keratinocyte pluripotent cells; b) stratum spinosum, composed of several layers of polyhedral keratinocytes; c) stratum granulosum, the granular layer with distinct keratohyalin granules visible in conventional electron microscopy; d) stratum corneum, consisting of dead corneocytes embedded in an intercellular lipid matrix (McGrath et al., 2004) (Fig. 1).

The epidermis contains no blood vessels and cells in the deepest layers of the epidermis are almost exclusively nourished by diffusion. Cells are formed through mitosis at the basal layer, stratum basale, and move up the strata changing shape and composition. Finally they reach the stratum corneum and are shredded by desquamation. This whole process is called epidermal differentiation (Eckhart et al., 2013). The turnover rate of the living epidermis is approximately 30-40 days (Weinstein et al., 1984). For the stratum corneum this process takes about 14 days (Jansen et al., 1974).

1.1.2 Stratum granulosum

Keratinocytes migrating up from the stratum spinosum has become known as granular cells, because of the distinct granular appearance of the cytoplasm in stained histological samples. These cells contain so-called keratinohyalin granules, which contain keratin-associated proteins (Sugiura et al., 2007). The granular, organelle-like appearance of keratinohyalin granules is a morphological artifact (Norlén and Al-Amoudi, 2004).

Like all the layers of the epidermis, except for the stratum corneum, cells of the stratum granulosum are held together by desmosomes. Desmosomes are highly organized disk-shaped junctions that serve as tethers for keratin intermediate filaments. Together with the attached intermediate filament network desmosomes form an intercellular scaffold that keeps cells together and distributes mechanical stress (Green and Simpson, 2007). Besides being an adhesive structure numerous studies have shown that desmosomes also have an important role in cytoskeletal organization, cell signaling and cell differentiation (Kottke et al., 2006).

Other characteristic structures for this layer are lamellar bodies (also called lamellar granules, membrane-coating granules, Odland bodies) (Matolsty, 1966; Odland et al., 1981; Landmann, 1986). Lamellar bodies play a key role in the skin barrier formation process by delivering lipids produced inside the keratinocytes to the extracellular space between the stratum granulosum and stratum corneum. With this process the keratinocytes of the stratum granulosum are actively involved in skin barrier formation.

Lamellar bodies are secretory organelles that have a unique biochemical composition and a multilamellar structure. Lamellar bodies are derived from the trans-Golgi network (Sakai et al., 2007, Tarutani et al., 2012). They contain cholesterol, phospholipids, glucoceramides, and sphingomyelin. Besides lipids lamellar bodies also contain a wide variety of enzymes and

2

peptides like glucocerebrosidase, acidic lipases and beta-defensin 2 (Feingold et al., 2014). In two-dimensional electron micrographs the lamellar bodies appear as vesicle-like membrane-bound organelles with a diameter of 0,2 – 0,3 μm (Feingold et al., 2014). The three-dimensional ultrastructure of the lamellar bodies has been subject for debate for half a century.

Two models have been proposed to describe the lamellar body system: The Landmann model (Landmann, 1986) and the membrane-folding model (Norlén, 2001). The Landmann model proposes that the lamellar body system is composed of numerous discrete vesicles that excrete their content to the extracellular space by fusion with the plasma membrane (Landmann, 1986). The Landmann model describes lamellar bodies as vesicles filled with smaller flattened vesicles termed lamellar disks that are excreted by exocytosis. In the extracellular space these lamellar disks fuse and form the lamellar pattern of the extracellular lipids. In contrast the membrane-folding model advocates that lamellar bodies consist of a single and coherent tuborectricular membrane network. This model further proposes that the lipids are excreted, via the single and coherent tuborectricular membrane network, as a tightly folded (cubic-like) lipid bilayer phase and that, once in the extracellular space, the lamellar pattern of the extracellular lipids is formed via a cubic-to-lamellar phase transition ("unfolding") of the lipid bilayer phase (Norlén, 2001).

1.1.3 Stratum corneum

The stratum corneum, also called the horny layer, is composed of about 20 layers of flat, hexagonal cells that partly overlap and have a thickness of approximately 0,3-0.5 μm and a diameter of approximately 30-60 μm (Menon et al., 2012). These cells are cornified keratinocytes, also called corneocytes, filled with mainly keratin and filaggrin, and contain no nuclei or organelles. The extracellular space between the cells is filled with stacked lipid bilayers with a line spacing of approximately 6,5 and 4,5 nm (Iwai et al., 2012). The lipids are delivered as hydrated bilayers of cholesterol, free fatty acids and glycosylceramides in the hairpin chain conformation, which subsequently undergo dehydration and deglycosylation (Holleran et al., 1993; Caspers et al., 2001). Together the corneocytes and the lamellar lipids are responsible for the skin barrier function (van Smeden et al., 2013).

Keratinocytes from the stratum granulosum terminally differentiate into dead corneocytes by a process called cornification and this process is associated with a reorganization of the keratin intermediate filament network (Al-Amoudi et al., 2004). Cornification includes two key steps, (1) the replacement of all the intracellular organelles and cytoplasm by a network of keratin and filaggrin, (2) the formation of the cornified envelope close to the plasma membrane by crosslinking of proteins recycled from the intracellular organelles, Together, these cornified cells form a multicellular, highly functional, but biologically dead, structure (Eckhart et al 2013).

After cornification approximately 80% of the cell mass of the stratum corneum consists of keratin, an α-helix enriched protein that forms coiled-coils (Pekny and Lane, 2007). The

keratin filaments are anchored in the cornified envelope and form a cubic-like rod packing as proposed by Norlén and Al-Amoudi (2004). The keratin filament organization forms an internal reinforcement securing shape and stability of the corneocyte like steal rods in re-enforced concrete. Besides keratin corneocytes contain larges amounts breakdown products of filaggrin, a protein that is thought to be responsible for aggregation of the keratin filaments, through a meganism that is still not properly understood (Sandilands et al., 2009).

Corneocytes are held together laterally by modified desmosomes called corneodesmosomes. At the interface between stratum granulosum and stratum corneum desmosomes differentiate into corneodesmosomes, where the desmosomal membrane complex contributes to the cornified envelope (Green and Simpson, 2007). Impairment of the degradation process of the corneodesmosomes influences the total thickness of the stratum corneum and can result in barrier deficiency (Ishida-Yamamoto et al., 2011).

The corneocytes are embedded in a lipid matrix. This lipid matrix consists of several lipid species that are transported from the stratum granulosum to the extra cellular space of the stratum corneum by the lamellar body system. The most abundant lipid species in the stratum corneum are ceramides, cholesterol and free fatty acids that are present in an approximate 1:1:1 molar ratio (White et al., 1988; Wertz and Norlén, 2003) (Fig 2). These lipid species form stacked lamellar layers and contribute to the skin barrier function (van Smeden et al., 2013).
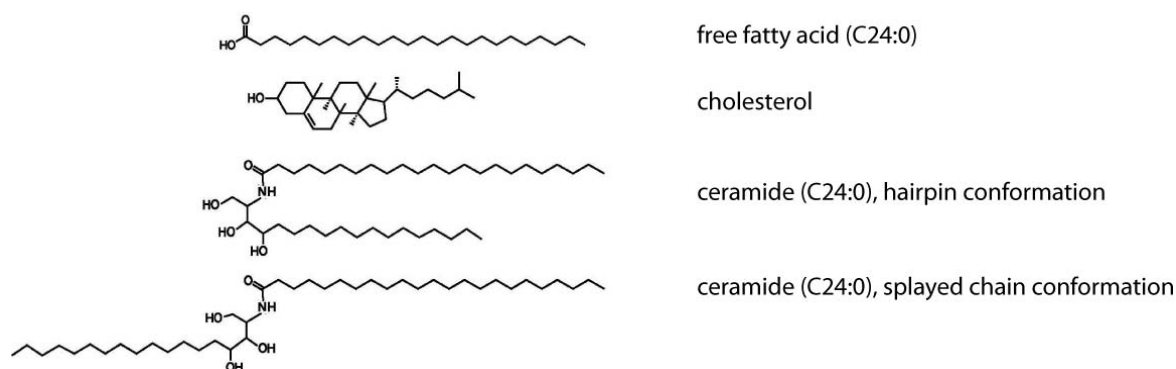

Fig 2. **The most abundant lipid species in the stratum corneum;** free fatty acid, cholesterol and ceramide.

1.2 THE SKIN BARRIER

The main function of the human skin is to create a barrier against environmental influences. The skin barrier is fundamental to terrestrial life and its evolution and sustains homeostasis and protects against the environment. This barrier is mainly established by lipids that fill the extracellular space of the uppermost layer of the epidermis, the stratum corneum (Elias, 1981). Lipids that are excreted via the lamellar body system (Rassner et al., 1999).

The structure and function of the human skin has been the subject of studies ever since the 1850's when Homolle (1853) and Duriau (1856) showed that the skin could absorb certain chemicals diluted in water. The next major breakthrough in skin barrier research was made by Winsor and Burch (1944) who discovered that the skin barrier actually is a function of the epidermal stratum corneum. This completely changed the perception of the dead stratum corneum, which was thought to be just a tough leathery layer to protect the skin from scratches and other damages. From that moment on skin barrier research focused on the epidermis and its uppermost layer, the stratum corneum. In the 1950's Berenson and Burch (1951) concluded that the inhibiting material in the stratum corneum must be lipids. Some 10 years later Brody (1966) discovered that the stratum corneum's intercellular spaces are filled with a non-homogeneous lipid-like substance. Electron microscopy studies in the early 1970's then revealed that the intercellular spaces are filled with lipids with a lamellar morphology (Breathnach et al., 1973, Elias and Friend, 1975).

1.2.1 Skin lipids and their organization

Ever since the discovery of the lamellar structure of the intercellular lipids by Breathnach et al. (1973) and Elias and Friend (1975) the molecular organization of these lamellar lipids has become an area of interest for many researchers.

One of the main problems encountered while studying the molecular organization of the lamellar lipids is the preservation of the stratum corneum lipids. Madison et al. (1987) made a break-through when introducing ruthenium tetroxide as a postfixation during the embedding of the stratum corneum for electron microscopy. They demonstrated that the lipid lamellae are arranged in a repeating broad-narrow-broad sequence of electron translucent bands (Madison et al., 1987; see also van den Bergh et al., 1997). Another widely used technique to address the lipids' molecular composition is X-ray diffraction. Using this approach White et al. (1988) observed a diffraction pattern with small angle X-ray diffraction of a series of small peaks indicating the presence of a lamellar phase with a periodicity of approximately 13 nm.

The information obtained form electron microscopy and X-ray diffraction studies has led to the proposition of several different models for the molecular organization of the molecular composition of lamellar lipids. Already during the 1980's Swartzendruber et al. (1989) proposed a model in which they suggested interlamellar sharing of lipid chains to produce lipid monolayers in between pairs of lipid bilayers. About five years later the "domain mosaic model" was proposed by Forslind (1994). This model suggests multiple, tightly packed domains composed of stratum corneum lipids in a crystalline state (i.e., with rigid lipid

chains) laterally separated by a continuous grain boarder phase composed of lipids in a liquid crystalline state (i.e., with fluid lipid chains). In 2001 the "sandwich model" (Bouwstra et al., 2001) and the "single gel phase model" (Norlén, 2001) were introduced, and followed by three additional models, based on electron microscopy (Hill and Wertz, 2003), X-ray diffraction (McIntosh, 2003) and neutron diffraction data (Schröter et al., 2009). Despite all these efforts it remained unclear how the lipids were organized on the molecular level. Understanding the physical structure of the lamellar lipids is crucial to understand the barrier function of the skin and ultimately to understand the mechanisms of barrier disruption in many skin diseases (Elias and Wakefield, 2014).

2 AIMS

The overall goal of this thesis was to elucidate the formation process and the molecular organization of the human skin barrier, as a disturbed skin barrier formation may be an important etiological factor in barrier deficient skin-disease such as eczema, psoriasis and the ichtyoses (Elias and Wakefield, 2014).

Paper 1 - To determine the basic molecular organisation of the human skin barrier, i.e., the skin's lipid matrix, in situ (Iwai et al., 2012).

Paper 2 - To resolve the key question of continuity vs. discreteness of the lamellar body system (den Hollander et al., 2016).

Paper 3 - To determine the basic formation of the skin barrier on the molecular level (den Hollander et al., 2016).

3   METHODS

3.1   SAMPLE PREPARATIONS

For all of our studies shave biopsies were taken form the mid part of the volar for arm and abdomen of 5 Caucasian males in their 40s – 50s with no history of skin disease. Biopsies were taken with a thickness of approximately 100 μm from each individual and immediately immersed in 1-hexadecene to avoid dehydration. They were cut up in small 1x1 mm pieces and placed in the cavity of a membrane carrier (Leica) filled with 1-hexadecene, and immediately vitrified using an EMPACT2 high pressure freezer (Leica). After the biopsy all the samples from each individual were vitrified within 20 minutes. After freezing the samples including the surrounding carriers were stored in liquid nitrogen until further use.

High pressure freezing (HPF) is able to cyo-immobilize biological samples by vitrification and is a way to overcome freezing damage. It consists of cooling water so rapidly that its molecules become immobilized before they can form crystals. This way it is possible to preserve the sample in its native state without the use of any fixatives. To accomplish vitrification with HPF the thickness of the sample must not exceed 200 μm (Dubochet et al., 1988).

3.2   ELECTRON MICROSCOPY

Electron microscopy is a versatile and useful tool to provide valuable insight into the ultrastructure of healthy and diseased skin. With electron microscopy it is possible to visualize very small structural details with high resolution with or without antibody labeling, in 2D and in 3D. We used electron microscopy for our main data collection in all our research.

3.2.1   Freeze-substitution serial section tomography

In order to obtain a 3D overview of the skin of an area of approximately 1500x1500x400 nm^3, we used freeze-substitution serial section tomography (FS-SET).

First, high pressure frozen samples were freeze-substituted by incubating them in methanol containing 2% GA + 0.5% uac + 1% OsO4 at -95°C for 10 hours, followed by -62°C for 8 hours and -40°C for 4 hours. After slowly heating the skin samples up to room temperature they were dehydrated in stepwise increased concentrations of acetone, embedded in LX-112 epon (Ladd research Industrustries, Wiliston, Vermont). For a general description of freeze-substitution of biological specimens, see Ikeda et al. (1984) and Weibul and Christiansson (1986).

After freeze substitution five ultrathin sections of approximately 80 nm thick were cut perpendicular to the skin surface using a diamond knife (Diatome). Each individual section was collected on a single-hole copper grid covered with Formvar and stained with uranyl acetate and Sato lead stain. The grids were placed in a dual axis tomography holder

(Fischione) and inserted into a Philips CM200 FEG electron microscope. Images were recorded with a pre-cooled slow scan 2048x2048 TVIPS TemCam-F224 HD CCD camera.

From each section a dual axis tomogram was generated from images recorded from exactly the same area of interest. For each tomogram, 240 images were collected from +70 to -70 degrees tilt angle, a magnification of 20.000, at a defocus of -0.5 micrometer and covering an area of approximately 1700 x 1600 nm^2. The two sets of data were combined and a dual axis tomogram was reconstructed with weighted back projection in IMOD. As a last step a series of consecutive dual dual axis tomograms were combined into a single serial section tomogram using the IMOD software.

Dual axis tomography increases resolution as it reduces the missing wedge in Fourier space to a missing pyramid. In particular, the primary effect of the missing wedge is to reduce the resolution in the Z direction. The missing wedge results in a severe loss of resolution for elongated structures that are oriented perpendicular to the tilt axis. In our studies we decided to use dual axis tomography whenever possible. For a general description of dual axis tomography, see Mastronarde (1997).

3.2.2 CEMOVIS

Cryo electron microscopy of vitreous sections (CEMOVIS) is a powerful tool in which the biological specimen is preserved in its near native state and every micrograph pixel's intensity is directly related to the local electron density of the specimen (Dubochet et al., 1988). Not only is it possible with this technique to visualize the skin in its near-native state, but also it is possible to visualize it with resolution below 1 nm.

The membrane carriers containing the vitreous skin samples were placed in the cryo-chamber of a pre-cooled Ultracut S microtome (Leica). The vitrified skin pieces were removed from the membrane carriers and placed into the sample holder of the microtome. The samples were trimmed with a diamond trimming knife (Diatome) and sectioned at -150 C^o with a nominal thickness of 30 to 50 nm using a 350 diamond knife (Diatome) with a clearance angle of 60 degrees and a cutting speed of 0.2-1.0 mm/s. Using an eyelash glued on a wooden stick the ribbons of sections were transferred to pre-cooled 1000 mesh copper grids and then pressed with a stamping tool. Grids with vitreous sections were transferred to a cryo-holder (GATAN) at -180 C^o and inserted into a Philips CM200 FEG electron microscope set to an acceleration voltage of 120kV.

More than five thousand images were recorded with a pre-cooled slow scan 2048x2048 TVIPS TemCam-F224 HD CCD camera at magnifications between 15.000 and 88.000, at a defocus between -0.5 μm – -3 μm, and with an electron dose between 3000-13000 $^{e-}$/nm^2.

To take images at a magnification of 50.000 - 88.000 without burning the precious area of interest we started at a low magnification (6.000X) where areas of interest were determined and the coordinates were stored in the microscope. At an uninteresting area the microscope was set to the desired magnification by going up stepwise in magnification focusing at every

magnification until the desired magnification was reached. At the desired magnification the sample was moved to one of the areas of interest and again focusing was performed. The sample was then moved one field of view out of the burnt focus area and a high quality image was taken. After acquiring an image the sample was again moved one field of view to perform the focusing step again. This was repeated until enough images were taken or all the areas of interest were exposed.

3.2.3 Tomography of vitreous sections

To visualize in 3D the membrane continuity between the plasma membrane and the lamellar bodies and between single lamellar bodies we used tomography of vitreous sections (TOVIS). In total three near-native skin sample volumes of about 1000x500x50 nm^3 were reconstructed in 3D.

The vitreous skin samples were sectioned at -150 C^o with a nominal thickness of 50 nm using a 35° diamond knife (Diatome) at a sectioning speed of 0.2-1.0 mm/s. Ribbons of sections were transferred to pre-cooled 600 mesh, thin bar, copper grids and pressed with a stamping tool. As fiducial markers PbS Core EviDots Espresso quantum dots (QDs) were used according to the method developed by Masich et al. (2006).

During our studies we have performed both single and dual axis TOVIS. For single axis TOVIS we transferred the copper grids to a pre-cooled cryo-holder (GATAN) and inserted into a Philips CM200 FEG electron microscope (Philips, Eindhoven, the Netherlands) set to an acceleration voltage of 200 kV, equipped with a pre-cooled slow scan 2048x2048 TVIPS TemCam-F224 HD CCD camera. Tilt series (n=12) from $+60^o$ to -60° with 1° increment were recorded at a defocus of -2 μm under low-dose conditions (in total approximately 4000 $^{e-/}nm^2$ per 120 image tilt-series) at a magnification of 20.000 and in an area of approximately 1600x1700 nm.

For dual axis TOVIS the copper grids were transferred to a pre-cooled cryo-holder (GATAN) that had been manually adapted by the Baumeister laboratory at the Max-Planck-Institute for Biochemistry in Martinsried, Germany and allow rotation of the grid 180 degrees inside the microscope and perform dual axis tomography. The first tilt series was collected similarly to single axis TOVIS. The low dose was, however, reduced to half the dose used for single axis TOVIS (in total approximately 2000 $^{e-}/nm^2$ per 120 image tilt-series, i.e. 4000 $^{e-}/nm^2$ per full dual axis tomogram). After collecting the first tilt series the sample was rotated 90 degrees, and a second tilt series was recorded under the same conditions.

The 3D reconstructions of both single and dual axis tomograms were performed by weighted back-projection and manual segmentation with the IMOD software package.

3.3 FOCUSED ION BEAM – SCANNING ELECTRON MICROSCOPY (FIB-SEM)

With an ultramicrotome (Leica) a small pyramid was prepared from each of two freeze substituted (FS) skin samples. The pyramid was cut from the skin sample block, mounted on a support stub of the FIB-SEM equipment and covered with a thick layer of conductive carbon, ensuring that the carbon made contact with the osmicated skin and improved conductivity. A 3 nm thick layer of platinum was deposited onto the sample with a sputter coater.

The samples were transferred to the FIB-SEM instrument (a FEI Nova Nanolab600 Dualbeam). To protect the area of interest from the ion beam and to prevent curtaining during cross sectioning, a local 1μm platinum layer was deposited on top of the sample.

Slices were milled in a sequential manner using an ion beam with a thickness of approximately 20 nm. The sample cross-sections obtained after each slice were then imaged in back-scatter electron mode using a 2.000 eV beam. For each data set, about 50 cross-sections were viewed.

The fifty consecutive 2D images were combined to a single 3D volume using ImageJ with the TomoJ plugin and manually aligned with IMOD. Lanczos resampling was used to lower the resolution of the aligned image stack. The Lanczos kernel is a time-limited approximation to the sinc function. The sinc function is theoretically optimal to use for resampling of band-limited signals, but has infinite support, i.e. extends to infinity. In practice, Lanczos filtering can be seen as being more contrast-preserving than Gaussian filtering, although some ringing artifacts can appear at strong edges in an image. Since our image data does not have discrete or very sharp edges at the original scale, Lanczos filtering is considered suitable. A resampled value is acquired by discrete convolution between the Lanczos kernel and the local image data around the position to be resampled. Resampling was performed with a down-sampling factor of 5.6.

The resampled volume was visualized using iso-surface rendering. The settings for the grey level were determined by measuring an easy distinguishable feature, like a lamellar body, in the original 2D image. The same feature in the reconstructed 3D volume was made to fit the corresponding features in the original 2D images by setting correctly the grey-scale intensity value. All the connected features were segmented using watershed segmentation (see below). Both the iso-surface rendering and segmentation were done in UCSF Chimera.

In total, three FIB-SEM data-sets were collected in three different areas from the two skin samples.

3.4 WATERSHED SEGMENTATION

To segment out all the connected structures in the density maps of our FS-SET and FIB-SEM datasets we used the watershed algorithm in Chimera. Before any segmentation was performed a Gaussian and median filtering was done and the correct grey level was

determined. The same features in the 3D volume were made to fit the 2D measurements, by varying with the grey-scale intensity value.

The watershed algorithm works as follows. If the considered voxel with a given density value is not adjacent to one or more voxels with the same or higher density value, it is assigned to a new region. When the considered voxel is adjacent to one or more voxels with the same or higher density value and the adjacent voxels are from one single region the considered voxel is assigned to that same region. If the considered voxel is adjacent to voxels from two or more regions, the regions are sorted by the number of adjacent voxels in each region in decreasing order; the considered voxel is then assigned to the highest region on the list. In this way the watershed algorithm traces by path growing all structures that are continuous with each other in 3D and assigns the same color to them.

3.5 ATOMIC MODELING

For two of our studies atomic models were reconstructed for a range of cubic and lamellar lipid phases. The atomic models include the three key components of the known lipid composition, namely ceramide NP (C18-phytosphingosine-non-hydroxy-C24:0), cholesterol and lignoceric acid (C24:0), because these will most likely determine the main features of the lipid organization, and variation in chain lengths will serve only to modulate the structure.

Models of the individual molecules were generated using a molecular model building procedure with the atoms being located at their ideal bond distances, angle and torsions. To obtain half stretched and fully stretched ceramides the molecule was rotated around the head group bonds $-CH(OH)-CH(CH_2OH)NH-$ and $-CH(CH_2OH)NH-COCH-$.

For further information about the modeling of the specific electron microscopic patterns see Iwai et al. (2012) and den Hollander et al. (2016).

3.6 CRYO-EM SIMULATION

From the generated atomic models simulated images were created with an electron microscopy simulation program developed by Rullgård et al. (2011). The first part of the program is a phantom generator that can read one or more atomic models in the RCSB Protein Data Bank (PDB) format and construct a model scenario with molecules at defined positions. From these model scenarios an electron scattering potential map is then generated with the background of vitrified water.

The second part of the program simulates the interaction between the potential map and the electron beam, the optical transformation effect of the lens system and the image formation on the detector. The parameters defining the optical properties of the microscope, like the acceleration voltage, aberration constants, defocus and the point spread function of the detector were set to mimic the real experiments. Thus, the simulated images were generated with conditions corresponding to the CEMOVIS images used in our studies

4 INTRACELLULAR TRANSPORT OF SKIN BARRIER LIPIDS VIA LAMELLAR BODIES

The skin barrier formation process is, although a lot of research has been done on this topic, still not properly understood. To understand the development of barrier-deficient skin disease, such as eczema and psoriasis, a better knowledge of the skin barrier function is crucial. Skin barrier formation can be divided into two important steps: lipid delivery to the extracellular space and lipid molecular reorganization. The first step in the skin barrier formation is the lipid excretion via the lamellar body system. This complicated cellular process transports lipids produced intracellularly into the extracellular space between the stratum granulosum and stratum corneum. Any aberration during this process may lead to barrier-deficient skin disease due to malformation of the intercellular lipid matrix.

Over time there are two different models proposed that describe the lamellar body system. The first published model suggests a multi-vesicular system filled with flattened lamellar disks that are excreted via a diffusion/fusion process (Landmann, 1986). More recently this model has been challenged and the membrane-folding model, that advocates that the lipid delivery takes place via a single and coherent tubulorecticular membrane system, has been proposed (Norlén, 2001). The lamellar body system has not previously been studied at high magnification in 3D and the question remains whether lamellar bodies observed in 2D electronmicrographs are 3-dimensional discrete vesicles or merely 2D-representations of a single tubulorecticular membrane network.

To discriminate between the 2 models several complementary 3D visualization techniques (TOVIS, FS-SET and FIB-SEM) were used in this thesis. As a near native high-resolution 2D reference CEMOVIS was used. Our data strongly favor the membrane-folding model (Norlén, 2001) and indicate the presence of a tubulorecticular membrane system. The TOVIS data shows membrane continuity in-between lamellar bodies and between lamellar bodies and the plasma membrane with a median diameter of 40.5 nm. Also the FS-SET and FIB-SEM data showed a low intensity tubulorecticular network that is continuous with the extra cellular space between the stratum granulosum and stratum corneum with a median diameter of 35 nm (FS-SET) and 70 nm (FIB-SEM). The low intensity tubulorecticular network found in FS-SET and FIB-SEM has similar dimensions as the lamellar bodies found in CEMOVIS and TOVIS. No discrete vesicles were observed in any of our 3D reconstructed skin samples obtained with TOVIS, FS-SET and FIB-SEM.

To determine membrane continuity in 3D, preservation of these membranes is crucial. The best preservation is obtained by methods using vitrification like TOVIS, where the sample is preserved in its near native state without any chemical fixation or extraction. Unfortunately, the 3D volume obtained from TOVIS is very limited due to the difficulty to collect vitreous sections and their sensitivity to handling and the electron beam (Dubochet et al., 1988, Sartori Blanc et al., 1998). With our microscope and sectioning equipment it was not possible to perform serial TOVIS to increase the 3D volume beyond the specimen single section

thickness of about 80 nm. Due to the limited 3D volume available, it was not possible with this particular technique to establish with certainty whether or not discrete vesicles are present.

To enlarge the 3D volume we performed FS-SET and FIB-SEM on freeze substituted samples. Although freeze substitution (FS) gives a better quality of ultrastructural preservation over conventional chemical preservation methods (Steinbrecht and Muller, 1987) and the use of acetone reduces the lipid extraction (Weibul et al., 1984), our results show signs of preservation artifacts. Lipid membranes were not always visible and stacked lamellar materials and multi-granular materials were not as abundantly present as in CEMOVIS and TOVIS and resulted in low intensity areas in electron micrographs. Despite the preservation artifacts, the low intensity signal did form a tubular network continuous with the extracellular space between stratum granulosum and stratum corneum. As shown with watershed segmentation, the network exhibited similar dimensions as that recorded in CEMOVIS and TOVIS. However, it cannot be excluded that other structures than lamellar bodies and transGolgi could have contributed to the low intensity signal.

The existence of a tubulorecticular network that is continuous with the extracellular space suggests that the lipid transportation to the extra cellular space does not proceed via a vesicular transport and fusion/diffusion process. This also implies that the intracellular organelles like the transGolgi network and mitochondria may be in close proximity to the extracellular space. This close proximity and the connection to the extracellular space may yield a flexible and fast reacting system for lipid and protein delivery to the intercellular space during skin barrier formation.

To our knowledge, this is the first published attempt to study the lamellar body system at high resolution in 3D, and a lot of challenges may lie ahead to confirm and expand this data. To get a more detailed and better view of the 3D structure of the tubulorecticular lamellar body system, better preservation is needed. Although the classical chemical fixation could be improved as exemplified by the use RuO4 in combination with osmium (van Smeden et al., 2013, Menon et al., 2014), it seems more attractive in future work to try to develop more automated cryo-electron microscopy- and cryo-sample handling procedures for serial-sectioning. Ideally ultrastructural microscopy methods should be combined with molecular cell biology methods to investigate the cellular processes and pathways involved in the lamellar body system, as has been done in alveolar cells (Miklavc et al., 2015).

5 FORMATION OF THE SKIN BARRIER EXAMINED ON A MOLECULAR LEVEL

The second step in skin barrier formation is the lipid molecular assembly. While lipids are transported via the lamellar body system into the extracellular space between the stratum corneum and stratum granulosum, they are bound to reorganize and adapt to their new location. During the transformation process we found five different characteristic high-resolution CEMOVIS patterns that correspond to five different steps in the lipid reorganization process (Fig 3).
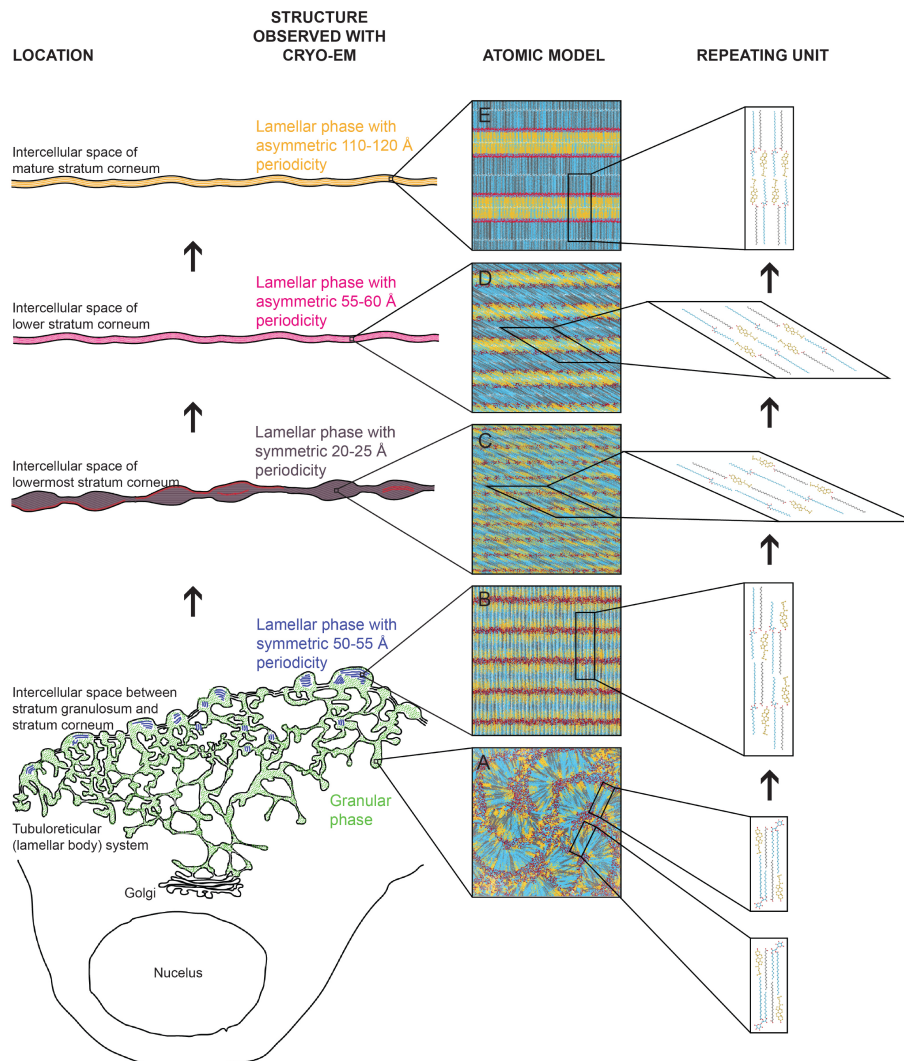
Fig 3. **Summary of the lipid reorganization steps taking place during formation of the stratum corneum lipid matrix.** A) 3D-folded lipid bilayer in hairpin chain conformation with cubic symmetry with a periodicity of ~ 15 nm. B) Stacked lamellar lipid bilayers in hairpin chain conformation with straight lipid chains, with no water between lipid leaflets, and with a periodicity of ~ 50-55 Å. C) tilted stacked lamellar lipid bilayers in hairpin conformation, with no water between lipid leaflets and with a periodicity of ~ 20-25 Å. D) tilted fully extended bilayers or non-tilted half-extended bilayers, with cholesterol associated with the ceramide sphingoid moiety, and with a periodicity of ~ 55-60 Å. E) Fully-extended bilayers in splayed chain conformation, with cholesterol associated with the ceramide sphingoid moiety, and with a periodicity of ~ 110-120 Å.

The first step is a cubic to lamellar phase transition (chapter 5.1) followed by the second step, a transformation to a splayed ceramide chain conformation (chapter 5.2). The third step comprises the tilting of the lipid chains (chapter 5.3) after which the ceramides, cholesterol and free fatty acids will change position through longitudinal displacement along the longitudinal axis (step 4) (chapter 5.4). In the final step (step 5) the lipids will straighten to a fully extended bilayer organization with lipids oriented perpendicular to the lamellar plane (chapter 5.5).

5.1 A CUBIC TO LAMELLAR PHASE TRANSITION

Inside lamellar bodies a tightly folded cubic-like lipid/water membrane with a ~ 15 nm periodicity is present and is the starting lipid matrix for the formation of the skin barrier. The cubic-like membranes are converted to multilamellar stacks of lipid layers with ~ 50-55 Å periodicity (Fig 3A).

Cubic membranes have been observed in numerous organisms and in a large amount of different cell types and organelles like chloroplasts in plants, mitochondria inner membranes in Xenopus testis cells and smooth endoplasmic reticulum in yeast (Land, 1995; Hyde et al., 1997; Almsherqi et al., 2006; Almsherqi et al., 2009). The cubic membrane configuration allows a most efficient packing of the highly curved lipid bilayers and provides high lipid mobility during transportation inside lamellar bodies due to its liquid crystalline state.

The most remarkable feature of the cubic membranes, the starting lipid matrix of the skin barrier, is their periodicity of approximately 15 nm, which is considerably shorter than the periodicity observed in cellular cubic membranes in other organisms (usually in the range of 50-500 nm according to Almsherqi et al. (2009). The periodicity of the cubic membranes recorded in human skin corresponds to the 10-30 nm periodicity of a thermodynamically stable cubic liquid/water phase (Larsson, 1989). This suggests that the cubic membranes observed in this study might have similar thermodynamically properties. It is not clear whether the observed 15 nm periodicity is unique for the skin barrier formation process or if it is observed here for the first time due to the use of high-resolution CEMOVIS.

The cubic-to-lamellar transition involves flattening of the folded bilayer while keeping the highly mobile liquid crystalline state (Larsson, 1994) and the removal of water from the lipid structure, which corresponds with the observation made by Caspers et al. (2001) that epidermis becomes dehydrated at the interface between stratum granulosum and stratum corneum and that the lipid sheets are completely dehydrated in the stratum corneum (Iwai et al., 2012). The cubic-to-lamellar transition requires very little energy, as emphasized by the low enthalpy difference between cubic and lamellar phases (Engström et al., 1992) as compared with the enthalpy difference between hexagonal and lamellar phases (Seddon et al., 1983). Due to this very low energy difference, transitions between cubic and lamellar phases may happen very easily, and may explain why lamellarization sometimes already start in the lamellar body system.

16

5.2 TRANSFORMATION TO SPLAYED CERAMIDE CHAIN CONFORMATION

In the absence of water the ceramides will convert from a hairpin to a fully splayed conformation resulting in a symmetric lamellar pattern with a periodicity of ~ 50-55 Å (Fig 3B). In crystals of phytosphingosine-based ceramides the splayed conformation is more energetically favorable than the hairpin conformation (Dahlén and Pascher, 1972). The dramatic reorganization of the ceramide conformation might thus be caused by the same reason; the stabilizing H-bonding system is shielded from the competition of water in a splayed conformation and thus better preserved.

5.3 TILTING OF THE LIPID CHAINS

When the deglycosylated ceramides are dehydrated, the saturated long-chain hydrocarbon tails will solidify into a gel-like state allowing restricted movements of the molecules. During this process the molecules become tilted and form a symmetric lamellar pattern with a ~ 20-25 Å periodicity (Fig 3C). The tilting process may be driven by the solidification process, which compensates for an energetically unfavorable arrangement of homogenously distributed ceramide sphingoid tails, ceramide fatty acid tails, cholesterol and free fatty acids by temporarily stabilizing the molecules in a metastable state due to the restricted mobility of the semi-solid ceramides.

5.4 LONGITUDINAL DISPLACEMENT OF CERAMIDE, CHOLESTEROL AND FREE FATTY ACIDS

During the metastable state the randomly distributed fully splayed ceramides, cholesterol and free fatty acids become organized into a stacked bilayer with the ceramide fatty acid tail pairing with free fatty acid and cholesterol with the ceramide sphingoid moiety giving different layers within the stacked bilayer structure. This process results in an asymmetric lamellar pattern with a ~ 55-60 Å lamellar periodicity (Fig 3D). The reorganization is dependent on several circumstances. Sliding along the molecules' length axes allows for an exchange between the adjacent layers without a dimensional change of the system as a whole. Cholesterol does not readily mix with fatty acids (Norlén et al., 2008), while it likes to pair with sphingosine and its derivatives (Garmy et al., 2005). In the tilted metastable state, the ill-matched C24 fatty acid and C18 sphingoid moieties, and the ill-matched cholesterol and long-chain saturated free fatty acids, might be a driving force for the sliding exchange along the lipid molecular axes.

5.5 STRAIGHTENING OF THE LIPIDS TO A FULLY EXTENDED BILAYER

To minimize the potential energy of the system the optimally arranged molecules straighten into an upright position creating a fully extended asymmetric lamellar pattern with a periodicity of 110-120 Å (Fig 3E).

6 MOLECULAR ORGANISATION OF THE SKIN BARRIER.

At the final stage of the skin barrier formation the lipid matrix is organized as asymmetrical stacked bilayers of fully extended ceramides with cholesterol associated to the ceramide sphingoid moiety. The asymmetrical stacked bilayers are characterized by a ~11 nm (10-12 nm) repeating unit consisting of alternating narrow (~4.5 nm) and broad (~6.5 nm) bands (Fig 4).

A) CEMOVIS micrograph

B) Averaged intensity profile along line pattern

C) Schematic 2D model
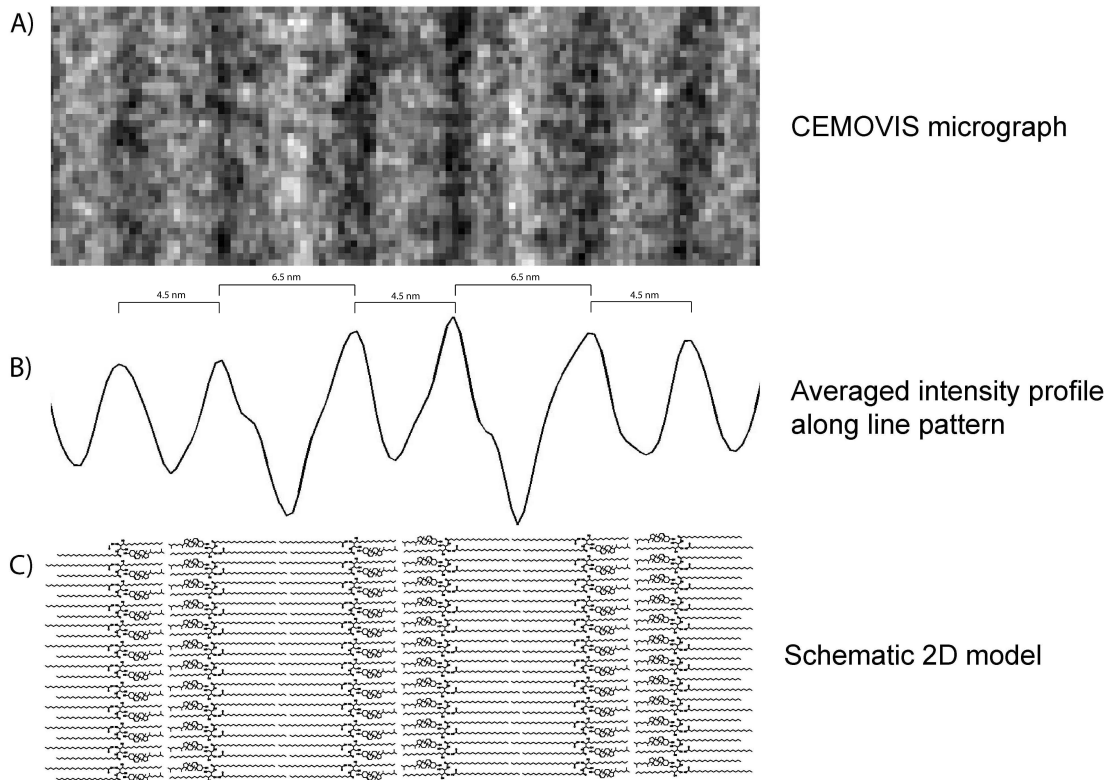
Fig 4. **The CEMOVIS intensity profile of the lipid matrix is characterized by an asymmetric ~11 nm repeating unit.** (A) High magnification CEMOVIS micrograph of the extracellular space in the midpart of stratum corneum. (B) Corresponding intensity profile. (C) Schematic 2D illustration of ceramides (tetracosanylphytosphingosine (C24:0)) in fully extended conformation with cholesterol associated with the ceramide sphingoid part and free fatty acids (lignoceric acid (C24:0)) associated with the ceramide fatty acid part.

The lipid molecules in the proposed lipid matrix (Fig 4) are packed optimally with the ceramide fatty acid tails pairing with free fatty acids of similar length (C24) and the cholesterol pairing with the ceramide sphigoid moieties (C14 – C18) matching the length of cholesterol (Ouimet and Lafleur, 2004). In model systems cholesterol does not mix with stratum corneum free fatty acids (Norlén et al., 2008), but has no problem mixing with sphingosine and its derivatives (Garmy et al., 2005). This asymmetrical packing results in the presence of alternating lipophilic (alkyl chain) and hydrophilic (headgroup) regions and will be largely impermeable to hydrophilic and lipophilic substances. In our studies we did not detect any water between the lipid leaflets. However this does not exclude a possible interaction between water and the extracellular lipids. Nakazawa et al. (2012) recorded

recently in an X-ray diffraction study a slight increase in the repeat distance of the lamellar lipid structure upon hydration. This emphasizes that the relationship between hydration, dehydration processes and the molecular lipid organization is still not fully understood.

The ~11 nm repeating unit found in our studies fits approximately with the 12-14 nm repeating unit observed in SAXD by White et al. (1988), Bouwstra et al. (1991), Hou et al. (1991), Schreiner et al. (2000) and Nakazawa et al. (2012) in isolated mice and human stratum corneum, as well as with the 12.9 nm repeating unit observed by Hou et al. (1991) in ruthenium tetroxide stained mice skin. The slight difference could be caused by differences in water content between the samples.

The formation of the ~11 nm repeating lipid matrix depends on the presence of all three lipids: ceramides, cholesterol and free fatty acids. Several skin diseases are characterized by an altered lipid organization as atopic dermatitis and ichthyosis (Pilgram et al., 2001). How this molecular organization is disrupted in these skin diseases is unknown. Ichthyosis appearing in inherited disorders of distal cholesterol metabolism (Elias et al., 2011) could offer an interesting possibility to study the structure of the barrier with no or reduced amounts of cholesterol present. In addition, pharmacological interference with the metabolism of cholesterol, ceramides and/or free fatty acids in mice (Feingold et al., 1990) could be explored to determine the effect of the essential lipid deployment.

It is well established that the extracellular space of the stratum corneum also contains non-lipids such as structural proteins derived from the lamellar body system, corneodesmosomes and the corneocyte envelope. Many of these proteins and complexes have been shown to contribute to the barrier function and most of them are related to a skin disease (Ishida-Yamamoto et al., 2011; Feingold, 2012). Some of these proteins might influence the barrier formation process, and some might affect the final organization of the barrier. All of them need to be investigated individually in the future.

7   CONCLUSIONS

1. Lamellar bodies are not discrete vesicles, but part of a tubulorecticular network continuous with the plasma membrane of stratum granulosum cells. The lipid excretion system can be regarded as a membrane folding/unfolding process and not as a lamellar body fusion process.

2. The lamellar lipid matrix is formed by five different steps:

       a) cubic- to lamellar membrane transition

       b) a hairpin- to splayed lipid chain transformation

       c) tilting of the lipid chains

       d) longitudinal displacement of ceramide, cholesterol and free fatty acids

       e) straightening of the lipids to a fully extended bilayer

3. The stratum corneum lamellar lipid matrix is organized in its final stage as stacked bilayers of fully extended ceramides with cholesterol associated to the sphingoid moiety.

8 ACKNOWLEDGEMENTS

look at slugs, bugs or beautiful stones that you find everywhere. You are a wonderful determined girl that makes everybody smile with your enthusiasm and openness. **Matthias,** my not so little boy, for all your hugs and kisses. Thank you for making me laugh with your cheeky smiles and your frolic adventures. You are such a happy, smart and curious boy and I hope you'll never stop asking "Why?"

9 REFERENCES

Al-Amoudi A, Norlén LPO, Dubochet J (2004) Cryo-electron microscopy of vitreous sections of native biological cells and tissues. *J Struct Biol* 148: 131-135.

Almsherqi ZA, Kohlwein SD, Deng Y (2006) Cubic membranes: a legend beyond the Flatland*of cell membrane organization. *J Cell Biol* 173: 839-844.

Almsherqi, ZA, Landh T, Kohlwein, SD, Deng Y (2009) Cubic membranes: the missing dimension of cell membrane organization. *Int Rev Cell Mol Biol* 274: 275-342.

Berenson GS, Burch GE (1951) Study of diffusion of water through dead human skin: the effect of different environmental states and of chemical alterations of the epidermis. *Am J Trop Med Hyg* 6: 842-853.

Brody I (1966) Intercellular space in normal human stratum corneum. *Nature* 209: 472 – 476.

Bouwstra JA, Gooris GS, Dubbelaar FER, Ponec M (2001) Phase behavior of lipid mixtures based on human ceramides: coexistence of crystalline and liquid phases. *J Lipid Res* 42: 1759-1770.

Caspers PJ, Lucassen GW, Carter EA, Bruining HA, Puppels GJ (2001) In vivo confocal raman microspectroscopy of the skin: noninvasive determination of molecular concentration profiles. *J Invest Dermatol* 116: 434-42.

Dahlén B, Pascher I (1972) Molecular arrangements in sphingolipids. Crystal structure of N-tetracosanoylphytosphingosine. *Chem Phys Lipids* 28: 2396-2404.

den Hollander L, Han HM, De Winter M, Svensson L, Masich S, Daneholt B, Norlén L (2016) Skin Lamellar Bodies are not Discrete Vesicles but Part of a Tubuloreticular Network. *Acta Derm Venereol* 96: 303-8.

Dubochet J, Adrian M, Chang JJ, Homo JC, Lepault J, McDowall AW Schultz P (1988) Cryo-electron microscopy of vitrified specimens. *Quart Rev Biophys* 21: 129-228.

Duriau F (1856) Recherches expérimentales sur l'absorption et l'exhalation par le tégument externe. *Arch Gen Med T* 7: 161-173.

Eckhart L, Lippens S, Tschachler E, Declercq W (2013) Cell death by cornification. *Biochim Biophys Acta* 1833: 3471-3480.

Elias PM (1981) Lipids and the Epidermal Permeability Barrier. *Arch Dermatol Res* 270: 95-117.

Elias PM, Crumrine D, Rodriguez-Martin M, Williams ML (2011) Pathogenesis of the cutaneous phenotype in inherited disorders of cholesterol metabolism: Therapeutic implications for topical treatment of these disorders. *Derm Endocrin* 3: 100-106.

Elias PM, Wakefield JS (2014) Mechanisms of abnormal lamellar body secretion and the dysfunctional skin barrier in patients with atopic dermatitis. *J Allergy Clin Immunol* 134: 781-791.

Engström S, Lindahl L, Wallin R, Engblom J (1992) A study of polar lipid drug carrier systems undergoing a thermoreversible lamellar-to-cubic phase transition. *Int J Pharm* 98: 137-145.

Feingold KR, Man MQ, Menon, GK, Cho SS, Brown BE, Elis PM (1990) Cholesterol synthesis is required for cutaneous barrier function in mice. *J Clin Invest* 86: 1738-45.

Feingold KR (2007) Thematic review series: Skin Lipids. The role of epidermal lipids in cutaneous permeability barrier homeostasis. *J Lipid Res* 48: 2531-2546.

Feingold KR (2012) Lamellar Bodies: The Key to Cutaneous Barrier Function. *J Invest Dermatol* 132: 1951-1953.

Feingold KR, Elias PM (2014) Role of lipids in the formation and maintenance of the cutaneous permeability barrier. *Biochim Biopys Acta* 1841: 280-294.

Fosklind BO (1994) A domain mosaic model of the skin barrier. *Acta Derm Venereol* 74: 1-6.

Garmy N, Taieb N, Yahi N, Fantini J (2005) Interaction of cholesterol with sphingosine: physicochemical characterization and impact on intestinal absorption. *J Lipid Res* 46: 36-45.

Green KJ, Simpson CL (2007) Desmosomes: New Perspectives on a Classic. *J Invest Dermatol* 127: 2499-2515.

Holleran WM, Takagi Y, Menon G, Legler G, Feingold KR (1993) Processing of epidermal glycosylceramides is required for optimal mammalian cutaneous permeability barrier function. *J Clin Invest* 91: 1656-64.

Homolle A (1853) Expériences physiologiques sur l'absorption par le tégument externe chez l'homme dans le bain. *Union Med* 7: 462.

Hyde S, Andersson S, Larsson K, Blum Z, Landh T, Lidin S, Ninham BW (1997) The language of shape. The role of curvature in condensed matter: physics, chemistry and biology. Elsevier Science B.V., Amsterdam.

Ikeda H, Ichikawa A, Ichikawa M (1984) The effects of freeze-substitution media on the infrastructure of inclusion bodies in type II pneumocytes of mouse lung processed by the cryofixation method. *J Electron Microsc* 33: 242-247.

Ishida-Yamamoto A, Igawa S, Kishibe M (2011) Order and disorder in corneocyte adhesion. *J Dermatol* 38: 1-10.

Jansen LH, Hojyo-Tomoko MT, Kligman AM (1974) Improved fluorescence staining technique for estimating turnover of the human stratum corneum. *Br J Dermatol* 90: 9-12.

Kottke MD, Delva E, Kowalczyk AP (2006) The desmosome: cell science lessons from human diseases. *J Cell Science* 119: 797-806.

Landh T (1995) From entangled membranes to eclectic morphologies: cubic membranes as subcellular space organizers. *FEBS Let* 369: 13-17.

Landmann L (1986) Epidermal permeability barrier: Transformation of lamellar granule-disks into intercellular sheets by membrane-fusion process, a freeze-fracture study. *J Invest Dermatol* 87: 202-209.

Larsson K (1989) Cubic Lipid-Water Phases: Structures and Biomembrane Aspects . *J Phys Chem* 93: 7304-7314.

Larsson K (1994) Liquid-crystalline lipid-water phases. Ch. 3 in Lipids - molecular organisation, physical functions and technical applications. 55-61 The Oily Press, Dundee, Scotland.

Madison KC, Swartzendrubr DC, Downing DT (1987) Presence of intact intercellular lipid lamellae in the upper layers of the Stratum Corneum. *J Invest Dermatol* 88: 714-718.

Masich S, Östberg T, Norlén L, Shupliakov O, Daneholt B. A procedure to deposit fiducial markers on vitreous cryo-sections for cellular tomography. *J Struct Biol* (2006) 156: 461-8.

Mastronarde DN (1997) Dual-axis tomography: an approach with alignment methods that preserve resolution. *J Struct Biol* 120: 343-52.

Matolsty AG (1966) Membrane-Coating Granules of the Epidermis . *J Ultrastruct Res* 15: 510-515.

McGrath JA, Eady RAJ, Pope FM (2004) Anatomy and organization of the Human skin. In: Rooks textbook of dermatology. Volume 1. (Burns T, Breathnach S, Cox N, Griffiths C eds) 3.1-3.84 Blackwell Science.

Menon GK, Cleary GW, Lane ME (2012) The structure and function of the stratum corneum. *Int J Pharmaceut* 435: 3-9

Menon GK, Orso E, Aslanidis C Crumrine D, Schmitz G, Elias PM (2014) Ultrastructure of skin from Refsum disease with emphasis on epidermal lamellar bodies and stratum corneum barrier lipid organization. *Arch Dermatol Res* 306: 731-737.

Miklavc P, Ehonger K, Sultan A, Felder T, Paul P, Gottschalk KE, Fick M (2015) Actin depolymerisation and crosslinking join forces with myosin II to contract actin coats on fused secretory vesicles. *J Cell Science* 128: 1193-1203.

Nakazawa H, Ohta N, Hatta I (2012) A possible regulation mechanism of water content in human stratum corneum via intercellular lipid matrix. *Chem Phys Lipids* 165: 238-243.

Norlén LPO (2001) Skin Barrier Structure and Function: The Single Gel Phase Model. *J Invest Dermatol* 117: 830-836.

Norlén L, Plasencia I Bagatolli L (2008) Stratum corneum lipid organization as observed by atomic force, confocal and two-photon excitation fluorescence microscopy. *Int J Cosmetic Science* 30: 391-411.

Odland GF, Holbrook K (1981) The lamellar granules of epidermis. *Curr Probl Dermatol* 9: 29-49.

Ouimet J, Lafleur M (2004) Hydrophobic match between cholesterol and saturated fatty acid is required for the formation of lamellar liquid ordered phases. *Langmuir* 20: 7474-7481.

Pekny M, Lane EB (2007) Intermediate filaments and stress. *Exp Cell Res* 313: 2244-2254.

Pilgram GSK, Vissers DCJ, van der Meulen H, Pavel S, Lavrijsen SPM, Bouwstra JA, Koerten HK (2001) Aberrant lipid organization in stratum corneum of patients with atopic dermatitis and lamellar ichthyosis. *J Invest Dermatol* 117: 710-717.

Proksch E, Brandner JM, Jensen JM (2008) The skin: an indispensable barrier. *Exp Dermatol* 17: 1063-1072.

Rassner U, Feingold KR, Crumrine DA, Elias PM (1999) Coordinate assembly of lipids and enzyme proteins into epidermal lamellar bodies. *Tissue & Cell* 31: 489-498.

Rullgård H, Öfverstedt LG, Masich S, Daneholt B, Öktem O (2011) Simulation of transmission electron microscope images of biological specimens. *J Microsc* 243: 234-256.

Sakai K, Akiyama M, Sugiyama-Nakagiri Y, McMillan JR, Sawamura D, Shimizu H (2007) Localization of ABCA12 from Golgi apparatus to lamellar granules in human upper epidermal keratinocytes. *Exp Dermatol* 16: 920-926.

Sandilands A, Sutherland C, Irvine AD, Mclean WJI (2009) Filaggrin in the frontline: role in skin barrier function and disease. *J Cell Science* 122: 1285-94.

Sartori Blanc N, Studer D, Ruhl K, Dubochet J (1998) Electron beam-induced changes in vitreous sections of biological samples. *J Microsc* 192: 194-201.

Seddon JM, Cevc G, Marsh D (1983) Calorimetric studies of the gel-fluid transition (Lb to La) and lamellar-inverted hexagonal (La to HII) phase transition in dialkyland diacyl-phosphatidylethanolamines. *Biochemistry* 22: 1280-1289.

Steinbrecht RA, Muller M (1987) Freeze substitution and freez-drying. Cryotechniques in biological electron microscopy. (ed. By RA Steinbrecht and K Zierold), 149-172. Springer-Verlag, Berlin.

Swartzendruber DC, Wertz PW, Kitko DJ, Madison KC, Downing DT (2010) Molecular models of the Intercellular Lipid Lamellae in Mammalian Stratum Corneum. *J Invest Dermatol* 92: 251-257.

Tarutani M, Nakajima, K, Uchida Y, Takaishi M, Goto-Inoue N, Ikawa M, Setou M, Kinoshita T, Elias PM Sano S, Meada Y (2012) GPHR-Dependent Functions of the Golgi Apparatus Are Essential for the Formation of Lamellar Granules and the Skin Barrier. *J Invest Dermatol* 132: 2019-2025.

Van den Bergh BAI, Swartzendruber DC, Bos-van der Geest A, Hoogstraate JJ, Schrijvers AHGJ, Bodde HE, Junginger HE, Bouwstra JA (1997) Development of an optimal protocol for the ultrastructural examination of skin by transmission electron microscopy. *J Microsc* 187: 125-133.

Van Smeden J, Janssens M, Gooris GS, Bouwstra JA (2014) The important role of stratum corneum lipids for the cutaneous barrier function. *Biochim Biophys Acta* 1841: 295-313.

Weibull C, Christiansson A (1986) Extraction of proteins and membrane lipids during low temperature embedding of biological material for electron microscopy. *J Microsc* 142: 79-86.

Weinstein GD, McCullouch JL, Ross P (1984) Cell Proliferation in Normal Epidermis. *J Invest Dermatol* 82: 623-628.

Wertz P, Norlén L (2003) "Confidence Intervals" for the "true" lipid compositions of the human skin barrier? In: Skin, Hair, and Nails. Structure and Function. (Forslind B, Lindberg M eds) 85-106 Marcel Dekker Inc.

White SH, Mirejovsky D, King GI (1988) Structure of lamellar lipid domains and corneocyte envelopes of murine stratum corneum. An X-ray diffraction study. *Biochem* 27: 3725-32.

Winsor T, Burch GE (1944) Differential roles of layers of human epigastric skin on diffusion rate of water. *J Intern Med* 74: 428-436.